

ORIGINAL ARTICLE

Establishment of practical recellularized liver graft for blood perfusion using primary rat hepatocytes and liver sinusoidal endothelial cells

Hidenobu Kojima¹ | Kentaro Yasuchika¹ | Ken Fukumitsu¹ | Takamichi Ishii¹ | Satoshi Ogiso¹ | Yuya Miyauchi¹ | Ryoya Yamaoka¹ | Takayuki Kawai¹ | Hokahiro Katayama¹ | Elena Yukie Yoshitoshi-Uebayashi^{1,2} | Sadahiko Kita¹ | Katsutaro Yasuda^{1,2} | Naoya Sasaki¹ | Junji Komori¹ | Shinji Uemoto¹

¹Department of Surgery, Graduate School of Medicine, Kyoto University, Kyoto, Japan

²Center for iPS Cell Research and Application (CiRA), Kyoto University, Kyoto, Japan

Correspondence

Kentaro Yasuchika
Email: kent@kuhp.kyoto-u.ac.jp

Funding information

Japan Society for the Promotion of Science, Grant/Award Number: 15K15065

Tissue decellularization produces a three-dimensional scaffold that can be used to fabricate functional liver grafts following recellularization. Inappropriate cell distribution and clotting during blood perfusion hinder the practical use of recellularized livers. Here we aimed to establish a seeding method for the optimal distribution of parenchymal and endothelial cells, and to evaluate the effect of liver sinusoidal endothelial cells (LSECs) in the decellularized liver. Primary rat hepatocytes and LSECs were seeded into decellularized whole-liver scaffolds via the biliary duct and portal vein, respectively. Biliary duct seeding provided appropriate hepatocyte distribution into the parenchymal space, and portal vein-seeded LSECs simultaneously lined the portal lumen, thereby maintaining function and morphology. Hepatocytes co-seeded with LSECs retained their function compared with those seeded alone. Platelet deposition was significantly decreased and hepatocyte viability was maintained in the co-seeded group after extracorporeal blood perfusion. In conclusion, our seeding method provided optimal cell distribution into the parenchyma and vasculature according to the three-dimensional structure of the decellularized liver. LSECs maintained hepatic function, and supported hepatocyte viability under blood perfusion in the engineered liver graft owing to their antithrombogenicity. This recellularization procedure could help produce practical liver grafts with blood perfusion.

KEYWORDS

animal models: murine, artificial organs/support devices, basic (laboratory) research/science, cellular biology, liver transplantation/hepatology, tissue/organ engineering

Abbreviations: 3D, three-dimensional; ANOVA, analysis of variance; BD, biliary duct; DPPIV, dipeptidyl peptidase-4; ECM, extracellular matrix; EGTA, ethylene glycol-bis-(β -aminoethyl ether)-N,N,N',N'-tetraacetic acid; ELISA, enzyme-linked immunosorbent assay; GFP, green fluorescent protein; H&E, hematoxylin and eosin; HUVECs, human umbilical vein endothelial cells; iPSCs, induced pluripotent stem cells; IVC, inferior vena cava; LSECs, liver sinusoidal endothelial cells; PBS, phosphate-buffered saline; PFA, paraformaldehyde; PV, portal vein; SEM, standard error of the mean; TUNEL, terminal deoxynucleotidyl transferase-mediated dUTP nick end-labeling; UGT1A1, UDP, glucuronosyltransferase 1 family, polypeptide A1.

© 2018 The American Society of Transplantation and the American Society of Transplant Surgeons

1 | INTRODUCTION

Liver transplantation is the only curative and established treatment for end-stage liver disease. However, patients who could benefit from this successful procedure are restricted by a severe donor organ shortage. Although alternative methods such as cell transplantation and bioartificial livers have been explored, these treatments have not yet substituted liver transplantation due to their limited efficacy.^{1,2} Thus engineering a transplantable and functional liver represents an attractive strategy to resolve these problems.

Decellularized liver scaffolds have recently been reported for application in whole-liver engineering.³⁻⁵ The decellularized three-dimensional (3D) liver scaffold consists of an extracellular matrix (ECM) forming a microvasculature for nutrient and gas transport, and molecules that may promote cell attachment and tissue generation.^{6,7} A decellularized liver scaffold is a promising material for tissue engineering; however, no clinically relevant recellularized liver graft has yet been achieved. In addition to the lack of abundant cell sources to ensure sufficient and effective recellularization, the main challenges include an inappropriate cell distribution in the complex 3D liver scaffold and clotting during blood perfusion, which lead to insufficient liver function *in vivo*. Therefore, efficient reestablishment of the parenchyma and vasculature needs to be achieved to produce a functional and transplantable recellularized liver.

In previous studies, the portal vein (PV) was used primarily as a seeding route for parenchymal cells.^{3-5,8} However, mechanical stress caused by the perfusate is inevitable, lasting several days during the migration process of recellularized cells into the parenchymal space.³ In addition, parenchymal cells seeded via the PV disturb portal blood flow into the portal lumen, and prevent the engraftment of endothelial cells along the vasculature. We have previously reported the efficient repopulation of parenchymal cells through the biliary duct (BD).⁹ Because of direct contact between the parenchymal space and the biliary tree, BD seeding of parenchymal cells represents an appealing method not only to avoid injury caused by the pressure of the perfusate on the PV, but also to maintain the portal lumen, which can then be used as a seeding route for endothelial cells to prevent clotting during blood circulation.

Several studies attempting the transplantation of a recellularized liver *in vivo* have demonstrated blood clotting in the scaffold.^{4,10-12} Clotting in the vasculature of a decellularized liver is a serious issue for its practical use *in vivo*. To control clotting and blood leakage into the parenchymal space, the bare lumen of the vasculature must be covered with endothelial cells. Thus far, various endothelial cells such as rat cardiac microvascular endothelial cells, human umbilical vein endothelial cells (HUVECs), MS1 cells, and endothelial progenitor cells have been described as potential cell sources for re-endothelialization.^{3,4,11,13} Liver sinusoidal endothelial cells (LSECs), which constitute part of the nonparenchymal cells in the liver, have not yet been reported as a potential source for this purpose. However, in addition to providing a physical barrier between hepatocytes and blood, LSECs serve also as scavenger cells, immune cells, and regulatory cells

interacting with hepatocytes.¹⁴⁻¹⁸ These functions suggest their great value for fabricating the vasculature in an engineered liver.

To produce functional liver grafts for blood perfusion, we developed a new seeding method for the optimal distribution of parenchymal cells with BD seeding and of endothelial cells with PV seeding in the decellularized liver, and evaluated the effect of LSECs in fabricating the vasculature in an engineered liver graft.

2 | MATERIALS AND METHODS

2.1 | Animals

Male Lewis rats or transgenic rats carrying the green fluorescent protein (GFP) gene (SLC, Hamamatsu, Japan) weighing 250-300 g were used for preparing the 3D liver scaffold and primary cell isolation. Male Lewis rats (SLC) weighing approximately 400 g were used for extracorporeal perfusion. The rats were maintained on a standard laboratory diet and water *ad libitum*, and were housed in a temperature- and humidity-controlled environment under a constant 12-hour light/dark cycle in the animal facility at Kyoto University. All animal experiments were approved by the Kyoto University Animal Experimentation Committee and were performed in accordance with Kyoto University Animal Protection Guidelines.

2.2 | Liver harvest and decellularization

Liver harvesting and preparation of the 3D liver scaffold were performed according to our previous report.⁹ In brief, the harvested liver previously cannulated with a 24-gauge cannula in the BD and an 18-gauge cannula in the PV was washed with phosphate-buffered saline (PBS). Subsequently, the liver was perfused with a 0.02% trypsin/0.05% ethylene glycol-bis-(β -aminoethyl ether)-N,N,N',N'-tetraacetic acid (EGTA) solution at 37°C for 1 hour at a flow rate of 1 mL/min to detach cells from the ECM, followed by perfusion with a detergent solution (1% Triton X-100/0.05% EGTA) for 18-24 hours at a flow rate of 1 mL/min to decellularize the organ. The decellularized liver was sterilized with 0.1% peracetic acid perfusion for 2 hours, followed by washing with PBS.

2.3 | Isolation of primary hepatocytes and LSECs

Hepatocytes were obtained using a 2-step collagenase perfusion technique as described previously,¹⁹ and LSECs were isolated by Percoll centrifugation with minor modifications.^{18,20} Details of the cell isolation procedure are provided in Supporting Information and Figure S1.

2.4 | Recellularization and re-endothelialization of liver scaffolds

A decellularized liver scaffold was placed in a 100-mm culture dish and then perfused with 20 mL of co-culture medium for

hepatocytes and LSECs through the PV prior to recellularization. The co-culture medium consisted of RPMI 1640 medium (Sigma-Aldrich, St. Louis, MO) with 10% fetal calf serum (ICN, Aurora, OH), 0.6 $\mu\text{g}/\text{mL}$ insulin (MP Biomedicals, Santa Ana, CA), 10 ng/mL VEGF (R&D, Minneapolis, MN, USA), 10 ng/mL epidermal growth factor (PeproTech, London, UK), 100 U/mL penicillin G and 100 $\mu\text{g}/\text{mL}$ streptomycin (Meiji Seika, Tokyo, Japan), 20 $\mu\text{g}/\text{mL}$ gentamycin (Sigma-Aldrich), and 50 ng/mL amphotericin B (Wako, Osaka, Japan). For recellularization into the parenchymal space, we introduced a total of 3×10^7 hepatocytes suspended in 30 mL of the culture medium into the scaffold through the BD. For re-endothelialization into the vasculature, a total of 1.5×10^7 LSECs or HUVECs suspended in 3 mL of the culture medium was injected into the scaffold through the PV. We seeded rat hepatocytes at a dose sufficient to be distributed in each lobe of the whole-liver scaffold, and LSECs at a quantity sufficient to cover the portal lumen including microvasculature. At each step, we injected the cell suspension into the scaffold at a flow rate of 1 mL/min.

2.5 | Perfusion culture of the recellularized liver graft

After 3 hours of static culture for cell attachment, we transferred the recellularized liver graft into a customized chamber for in vitro perfusion culture. The cannula inserted into the PV of the recellularized liver graft was connected to a recirculation circuit and continuously perfused with the co-culture medium for 1 week using a peristaltic pump at a sub-physiological flow rate of 0.5 mL/min, to attenuate shear stress to seeded hepatocytes, as described previously.⁹ The medium was changed every 48 hours, and samples were obtained to analyze protein secretion levels. Histological analysis of the cultured recellularized livers was performed on day 2 and day 6 of perfusion culture.

2.6 | Extracorporeal blood perfusion of the recellularized liver graft

We placed the recellularized liver graft in the extracorporeal blood perfusion system using a live rat to evaluate the antithrombotic ability of endothelial cells and the feasibility of our recellularized liver for blood perfusion. The extracorporeal perfusion system incorporated with our fabricated liver graft (Figure S2) was established based on the circuit of an extracorporeal bioartificial liver.²¹ Under general anesthesia with isoflurane (Wako), cannulation of the left carotid artery and the right jugular vein was performed using a PE 50 polyethylene tube (Becton Dickinson and Co., Sparks, MD) and a 0.5×1 mm silicone tube (As One, Osaka, Japan), respectively. The circuit was primed with heparinized (10 units/mL) saline solution, and then after 2 days of perfusion culture, our fabricated liver graft was put in the extracorporeal perfusion system. The rats were administered 100 units heparin intravenously 5 minutes before the start of extracorporeal perfusion. To compensate for the dead volume of the circuit, 5 mL of fresh rat blood was transfused

immediately before perfusion. Subsequently, the arterial and venous lines were connected to the extracorporeal circuit. Arterial blood was pumped into the PV cannula inserted in the recellularized liver graft at a flow rate of 1.0 mL/min, which is slower than the physiological flow to minimize the shear stress to the engrafted cells. The blood through the liver graft was drained from the inferior vena cava (IVC) and returned to the jugular vein at the same flow rate by digital variable-speed infusion pumps (Top, Tokyo, Japan). During the perfusion, heparinized saline solution (40 units/mL) was continuously administered just before the recellularized liver graft at a flow rate of 0.3 mL/h to prevent coagulation in the graft and circuit due to blood perfusion. Histological analysis of liver grafts was performed after 3 hours of extracorporeal blood perfusion. The deposition of platelets was compared between the group co-seeded with hepatocytes and LSECs (Hep + LSEC), the group co-seeded with hepatocytes and HUVECs (Hep + HUVEC), and the group seeded with hepatocytes alone (Hep), by measuring the average fluorescence intensities of integrin αIIb (5 random periportal and central vein areas of 3 sections; $n = 3$ livers per group) using ImageJ software, as evaluated in previous reports.^{4,11}

2.7 | Scanning electron microscopy examination

Re-endothelialized liver grafts with LSECs after 2 days of perfusion culture were perfused with 2% glutaraldehyde and 4% paraformaldehyde (PFA) in PBS, and cut into 5-mm³ pieces. The samples were fixed in 2% glutaraldehyde and 4% PFA in PBS at 4°C overnight, and then ion-sputter-coated. Samples were observed with a Hitachi S-4700 scanning electron microscope (Hitachi, Tokyo, Japan).

2.8 | Liver function analysis

Albumin content in the medium was measured using a rat albumin enzyme-linked immunosorbent assay (ELISA) quantification kit (Bethyl Laboratories, Montgomery, TX). Urea content in the medium was analyzed using the QuantiChrom Urea Assay Kit (BioAssay Systems, Hayward, CA), according to the manufacturer's protocol. Total bile acids were measured by a standard spectrophotometric method with an automated analyzer (JEOL Ltd., Tokyo, Japan).

2.9 | Statistical analysis

Data are expressed as the mean \pm standard error of the mean (SEM). We performed statistical analyses using GraphPad Prism, version 6.0 (GraphPad Software, La Jolla, CA). Statistical significance was defined as $P < .05$. Terminal deoxynucleotidyl transferase-mediated dUTP nick end-labeling (TUNEL)-positive cells and deposition of platelets were compared using Student's *t*-test. The metabolic activity of recellularized liver grafts was compared using repeated-measures analysis of variance (ANOVA), followed by Bonferroni post hoc tests (additional information about the materials and methods is provided in Supporting Information).

3 | RESULTS

3.1 | Decellularization of the whole liver

An acellular whole-liver scaffold was obtained by portal perfusion after 24 hours of the decellularization procedure (Figure 1A). Histological analysis confirmed the lack of nuclei or cytoplasmic components in the decellularized liver scaffold (Figure 1B). Crystal violet staining confirmed that the PV and BD, serving as routes for recellularization, were retained and patent to the peripheral capillaries after decellularization (Figure 1C-F). The infused dye flowed out from the vasculature and distributed into the parenchymal space without leakage from the surface of the liver in the late phase of both PV (Figure 1D) and BD (Figure 1F) staining, and finally drained to the IVC.

3.2 | Recellularization of hepatocytes into the parenchymal space with BD seeding

Macroscopic observation of the liver recellularized with primary rat hepatocytes by BD seeding demonstrated that hepatocytes were distributed in each lobe of the whole-liver scaffold and spread outside of the biliary tree (Figure 2A). Hematoxylin and

eosin (H&E) staining of the recellularized liver graft on day 2 of perfusion culture revealed an appropriate cell distribution of the hepatocytes into the parenchymal space without intravascular embolus (Figure 2B). Immunohistochemical staining after 2 days of perfusion culture showed that albumin and UDP glucuronosyltransferase 1 family, polypeptide A1 (UGT1A1) expression in the recellularized liver was similar to that in the normal liver (Figure 2C). Furthermore, dipeptidyl peptidase-4 (DPP4) or CD26, a known marker of bile canaliculi, was detected in sections of the recellularized liver graft (Figure 2C). This result provides evidence that cell polarity of hepatocytes was organized in the engineered liver graft, possibly reproducing the channels through which bile acids were secreted.²²

3.3 | Re-endothelialization of LSECs into the vasculature with PV seeding

We injected LSECs by PV seeding after culturing them in the presence of VEGF for 5 days on a collagen-coated dish. Fluorescence microscopy showed GFP⁺ LSECs covering the microvasculature of the PV (Figure 3A). H&E staining on day 2 of perfusion culture demonstrated LSECs lining the portal lumen (Figure 3B,C), including parts where

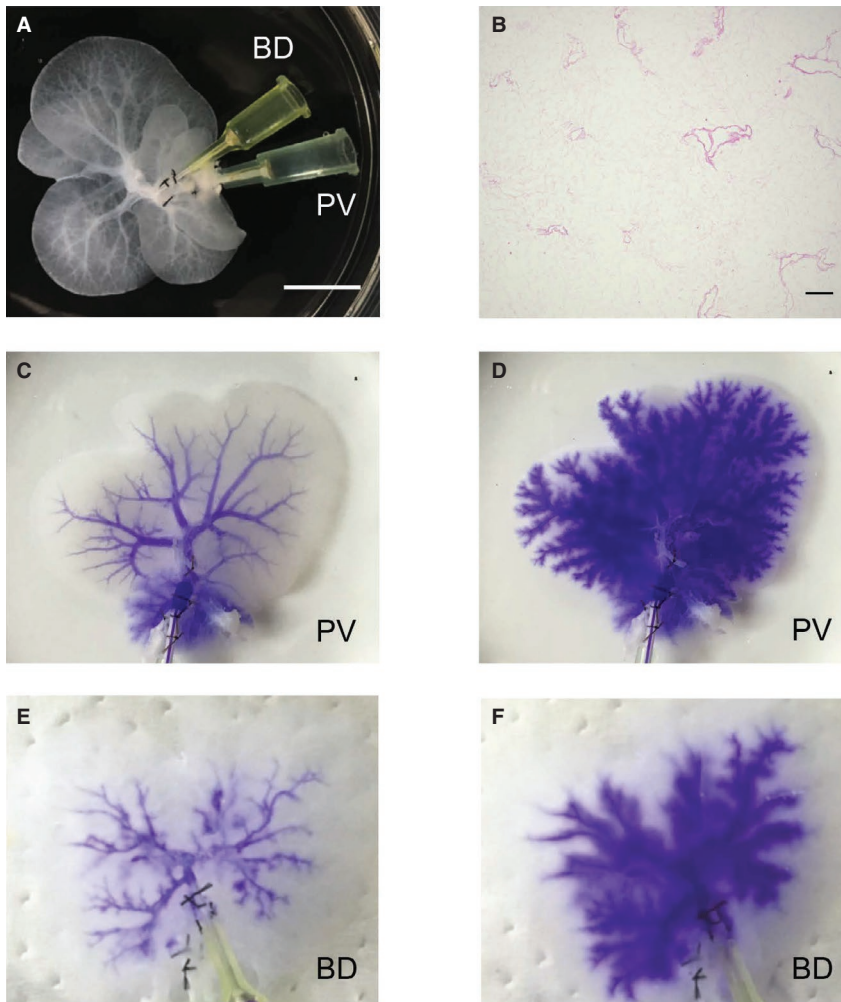
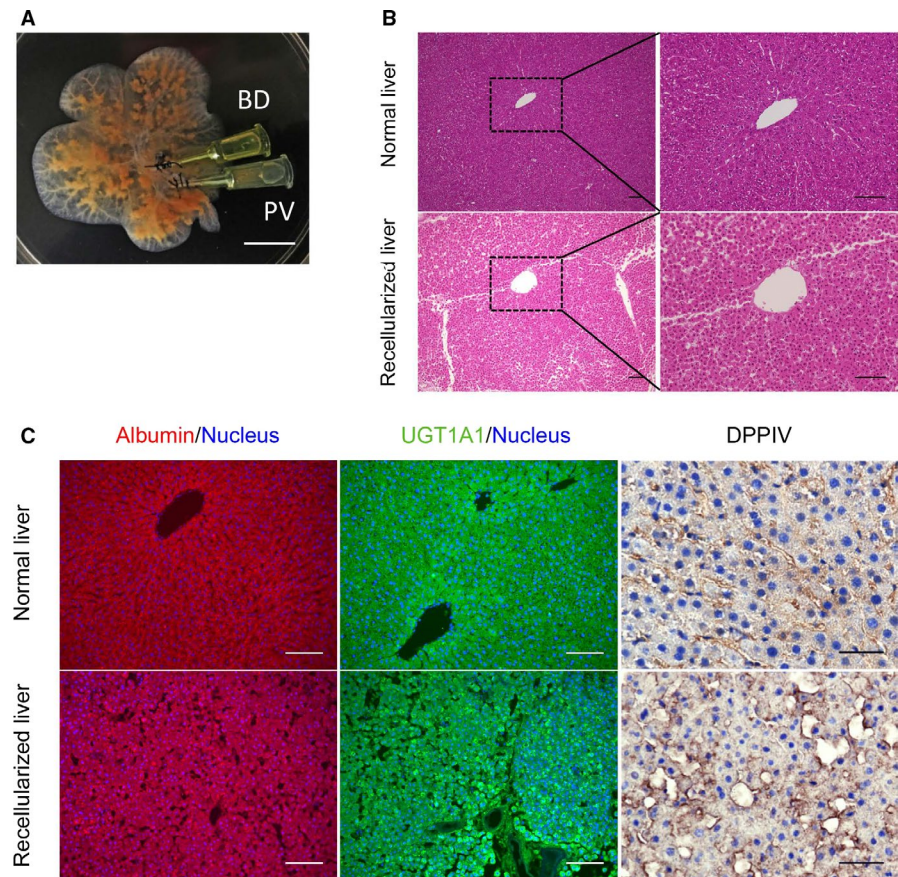


FIGURE 1 Preparation of the decellularized whole-liver scaffold and evaluation of the seeding route. (A) Acellular whole-liver scaffold cannulated into the portal vein (PV) and biliary duct (BD). (B) Hematoxylin and eosin staining of the decellularized liver showing no nuclei or cytoplasm in the scaffold. (C) PV dyeing with 300 μ L. (D) PV dyeing with 300 μ L. (E) BD dyeing with 300 μ L. (F) BD dyeing with 300 μ L. Scale bars = 10 mm (A) and 100 μ m (B) [Colour figure can be viewed at wileyonlinelibrary.com]

FIGURE 2 Recellularization of hepatocytes into the parenchymal space with biliary duct (BD) seeding. (A) Macroscopic observation of the recellularized liver following BD seeding of hepatocytes. (B) Hematoxylin and eosin staining of the normal liver (top) and recellularized liver on day 2 of perfusion culture (bottom). (C) Immunohistochemical analyses of the normal liver (top) and recellularized liver on day 2 of perfusion culture (bottom) stained for albumin, UDP glucuronosyltransferase 1 family, polypeptide A1 (UGT1A1), and dipeptidyl peptidase-4 (DPPIV). DPPIV staining of the recellularized liver demonstrates hepatocyte polarity. Scale bars = 10 mm (A), 100 μ m (B, C; left and middle), and 40 μ m (C; right) [Colour figure can be viewed at wileyonlinelibrary.com]



cell-cell junctions of endothelial cells could be observed under higher magnification (Figure 3C, arrowheads). Scanning electron microscopy examination showed LSECs attached to the portal lumen of the decellularized liver, which retained their fenestrations to permit the selective passage of proteins and metabolites (Figure 3D). Furthermore, immunohistochemistry revealed sustained expression of the hepatic sinusoidal endothelial marker (SE-1) and stabilin-2, known biomarkers for the LSEC phenotype (Figure 3E). In contrast, expression of the ubiquitous endothelial marker CD31 on LSECs was very low (Figure 3E). We also detected almost no expression of other markers for hepatic nonparenchymal cells such as Kupffer cells or stellate cells in the liver scaffold seeded with LSECs (Figure S3). These results indicate that the characteristic phenotype and morphology of LSECs were well maintained and reproduced on the decellularized liver scaffold. We confirmed the completely opposite expression of SE-1, stabilin-2, and CD31 in HUVECs seeded in the same manner as LSECs (Figure 3E).

3.4 | Co-seeding of hepatocytes and LSECs: optimal cell distribution and maintenance of hepatic function

After recellularization of hepatocytes into the parenchymal space with BD seeding, we performed re-endothelialization of LSECs into the vasculature with PV seeding, and proceeded with perfusion culture for 1 week (Figure 4A,B). H&E staining on day 2 of perfusion

culture showed an appropriate cell distribution of hepatocytes into the parenchymal space and of LSECs into the portal vasculature (Figure 4C). Thus the hepatocytes recellularized via BD seeding did not obstruct the portal lumen, allowing for proper attachment of LSECs.

To assess the interaction between LSECs and hepatocytes, we compared metabolic activity between the Hep + LSEC and Hep groups during perfusion culture. Cumulative albumin secretion and urea synthesis levels were significantly higher in the Hep + LSEC group than in the Hep group ($P = .006$ and $.003$, respectively; Figure 5A,B). These results suggest that LSECs maintained hepatocyte function during the perfusion culture. Although total bile acids secretion levels were higher in the Hep + LSEC group than in the Hep group, the difference was not statistically significant ($P = .313$; Figure 5C). We further compared the metabolic activity between the Hep + HUVEC and Hep groups during the perfusion culture. Cumulative albumin secretion and urea synthesis levels were higher in the Hep + HUVEC group than in the Hep group; however, differences between groups were not statistically significant ($P = .068$ and $.516$, respectively; Figure 5A,B). Similarly, there was no statistically significant difference in total bile acid secretion levels (Figure 5C).

The numbers of TUNEL-positive cells among hepatocytes were higher in the Hep group than in the Hep + LSEC group on day 2 of perfusion culture, with a large disparity observed by day 6; however, differences between the groups were not statistically significant ($P = .408$ and $.100$, respectively; Figure 5D).

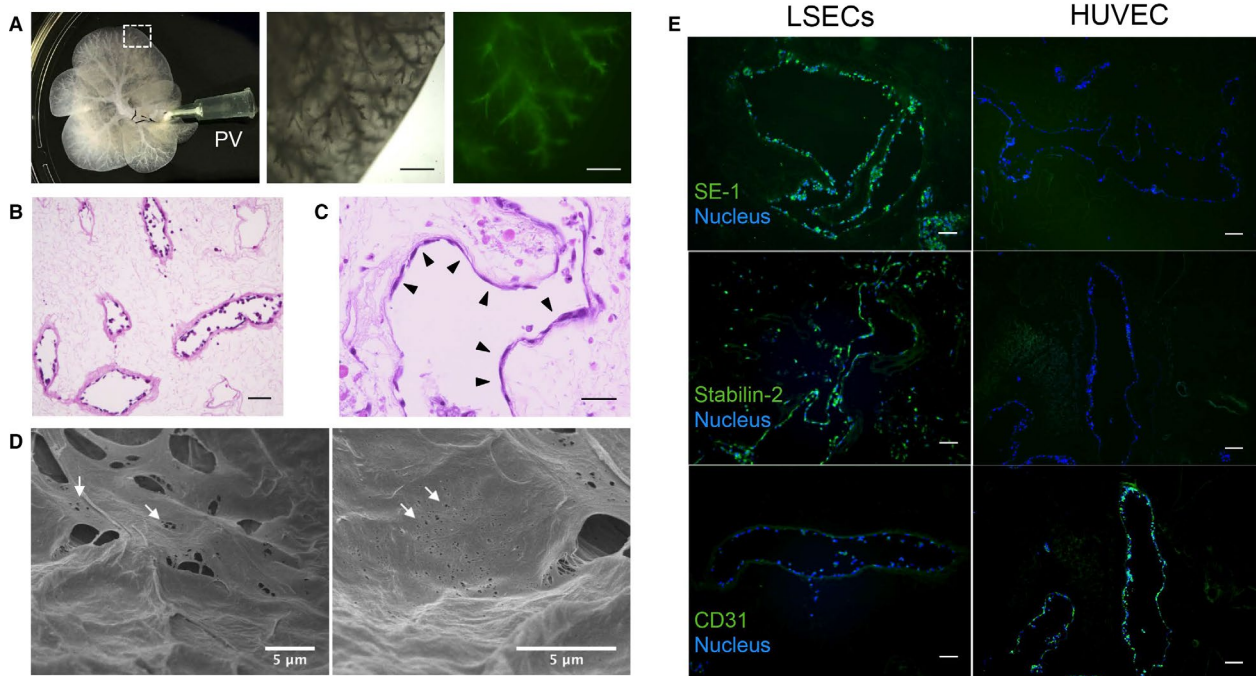


FIGURE 3 Re-endothelialization of LSECs and HUVECs into the vasculature with portal vein (PV) seeding. (A) Left: Macroscopic observation of the re-endothelialized liver with LSECs by PV seeding. Middle: Microscopic observation of the framed part of the macroscopic photograph. Right: Fluorescence microscopic observation in the same part; GFP⁺ LSECs covered the microvasculature of the PV. (B,C) Hematoxylin and eosin staining of the re-endothelialized liver on day 2 of perfusion culture. Arrowheads indicate cell-cell junction of endothelial cells. (D) Scanning electron microscopy examination of the re-endothelialized liver scaffold. Arrows indicate retained fenestrations. (E) Hepatic sinusoidal endothelial marker (SE-1), stabilin-2, and CD31 expression in LSECs and HUVECs on day 2 of perfusion culture. Scale bars = 1 mm (A), 100 μm (B), 40 μm (C), and 100 μm (E) [Colour figure can be viewed at wileyonlinelibrary.com]

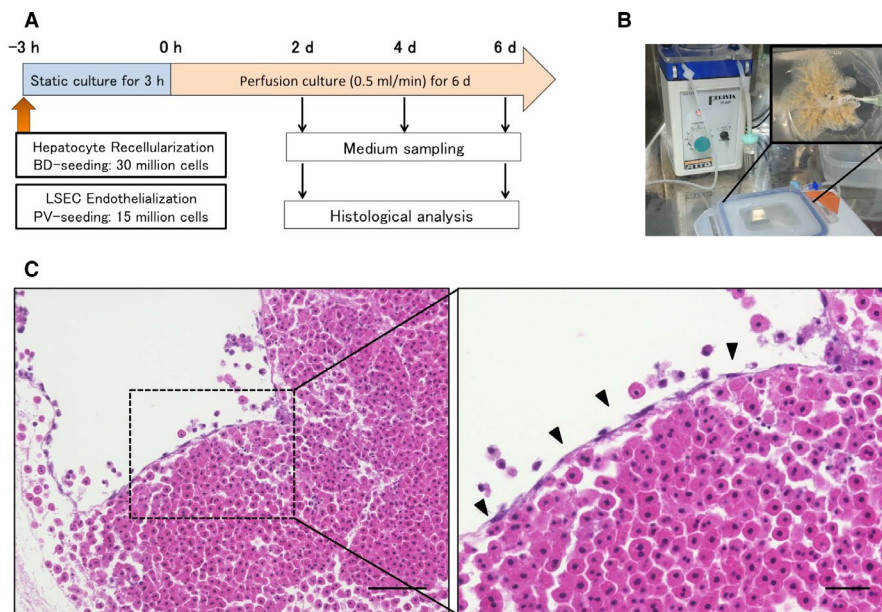


FIGURE 4 Co-culture of hepatocytes recellularized with biliary duct (BD) seeding and LSECs re-endothelialized with portal vein (PV) seeding. (A) Protocol for recellularization with hepatocytes and LSECs, and perfusion culture. (B) Recellularized liver grafts were connected to the recirculation circuit by a cannula inserted into the PV and were continuously perfused with co-culture medium. (C) Hematoxylin and eosin staining on day 2 of perfusion culture. Arrowheads indicate LSECs attached on the portal lumen. Scale bars = 100 μm (C; left) and 40 μm (C; right) [Colour figure can be viewed at wileyonlinelibrary.com]

3.5 | Evaluation of the engineered liver graft after extracorporeal blood perfusion

Following 2 days of perfusion culture, we placed the engineered liver grafts in an extracorporeal perfusion system (Figure 6A) and performed blood circulation into the liver graft for 3 hours. All of the rats tolerated the extracorporeal perfusion and no death was observed.

The blood filled into the scaffold in about 10 minutes via the PV and finally drained to the IVC (Figure S2). Although some clots were observed in the gross appearance of recellularized liver grafts after extracorporeal perfusion (Figure 6B-D), blood clotting that did occur in the liver grafts was not sufficiently severe to stop blood flow during extracorporeal perfusion in any of the Hep + LSEC, Hep + HUVEC, and Hep groups. Furthermore, PBS injected into the PV after extracorporeal

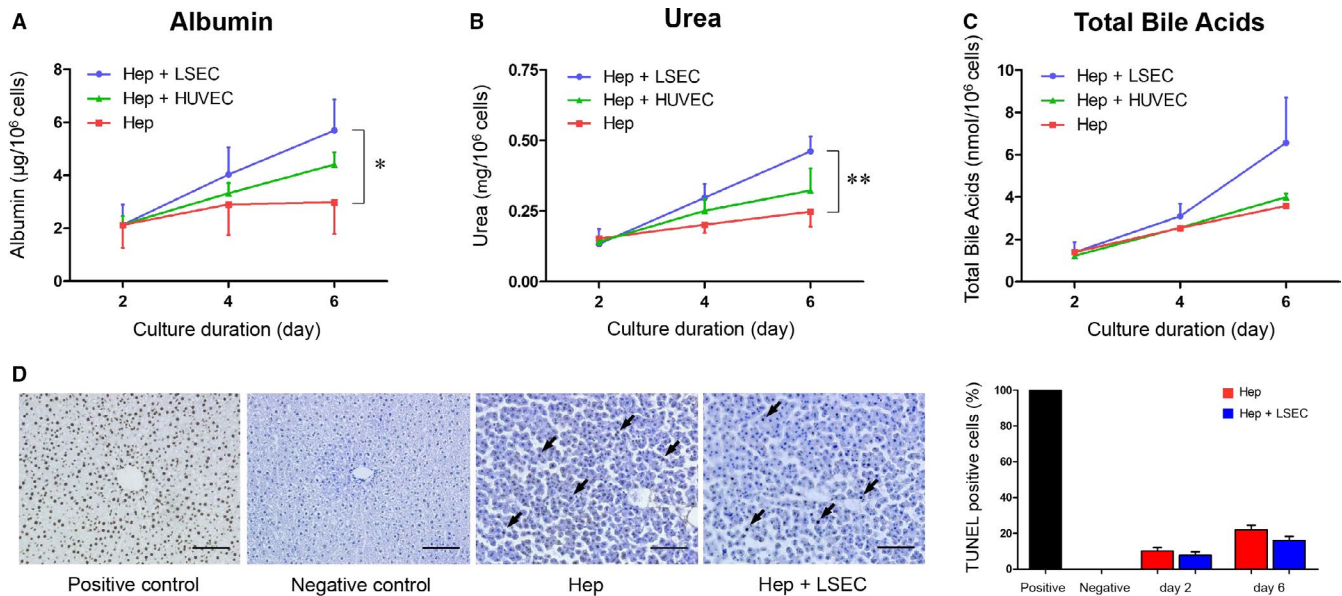


FIGURE 5 Comparison of metabolic activity and TUNEL-positive cells in hepatocytes with LSECs (Hep + LSEC), HUVECs (Hep + HUVEC), and cultured alone (Hep) during perfusion culture. Cumulative albumin secretion (A), urea synthesis (B), and total bile acids secretion (C). * $P = .006$ for albumin, ** $P = .003$ for urea, and $P = .313$ for total bile acids between the Hep + LSEC and Hep groups. $P = .068$ for albumin, $P = .516$ for urea, and $P = .087$ for total bile acids between the Hep + HUVEC and Hep groups. (D) TUNEL-positive cells (arrows), and their counts from day 2 to day 6 of perfusion culture in the Hep + LSEC and Hep groups. Scale bars = 100 μm (D). All error bars represent the standard error of the mean ($n = 3$) [Colour figure can be viewed at wileyonlinelibrary.com]

perfusion was drained to the IVC without obvious leakage from the surface of the recellularized liver, suggesting the presence of patent routes through which blood could flow; moreover, the polarity of perfusion from the PV to IVC was maintained. After extracorporeal blood perfusion, the liver graft of the Hep group (Figure 6B) showed a tendency to shrink compared with those of the Hep + LSEC and Hep + HUVEC groups (Figure 6C,D). This observation suggests that appropriate blood circulation could be maintained in the endothelialized liver grafts during extracorporeal perfusion.

Histological analysis revealed that several of the major portal lumens retained their patency, and LSEC functional SE-1 expression was maintained even after extracorporeal blood perfusion (Figure 6E, Figure S4). To evaluate the antithrombotic ability of endothelial cells, we quantified platelet deposition by measuring fluorescence intensity of integrin αIIb . The Hep + LSEC and Hep + HUVEC groups showed significantly reduced platelet deposition compared with the Hep group ($P < .001$; Figure 6F). Furthermore, the Hep + HUVEC group exhibited significantly lower platelet deposition than the Hep + LSEC group ($P < .001$; Figure 6F). At the same time, no significant difference between the 3 groups was observed in terms of platelet deposition in the central vein system, which was not re-endothelialized (Figure S5).

The number of TUNEL-positive hepatocytes increased after extracorporeal blood perfusion in all 3 groups, resulting in a significant difference between the Hep and Hep + LSEC groups, and between the Hep and Hep + HUVEC groups ($P = .027$ and $.004$, respectively; Figure 6G). These results indicated that, owing to their antithrombogenicity, LSECs and HUVECs might contribute to hepatocyte viability during blood perfusion in the engineered liver grafts. No significant difference in the number of TUNEL-positive hepatocytes

was detected between the Hep + LSEC and Hep + HUVEC groups (Figure 6G).

4 | DISCUSSION

Organ decellularization is a recently well-established and reproducible technique,^{3-5,8,11} allowing for a whole-liver decellularized scaffold to be obtained from rodent, porcine, or even human livers.^{8,11,23-25} Although engineered livers derived by decellularization were expected to regenerate transplantable liver grafts, no study has yet achieved its practical use in vivo. One of the essential issues for the practical use of decellularized liver grafts is establishment of an efficient recellularization technique to reconstruct the parenchyma and vasculature; however, the methods have not yet been optimized. Recently, we reported that BD seeding of parenchymal cells could achieve a more efficient cell distribution into the appropriate space compared with PV seeding.⁹ As shown in the present study, BD seeding of parenchymal cells can maintain the vasculature lumen empty to allow concomitant seeding of endothelial cells via the PV. Furthermore, we demonstrated cell polarity of hepatocytes using DPPIV staining in the recellularized liver. Our findings indicate that hepatocytes recellularized with BD seeding could effectively reconstruct the structural polarity and thereby might possess appropriate tight junctions in the parenchymal space. Thus parenchymal cells recellularized with BD seeding could maintain viability and function in their appropriate space.

Reconstruction of the vasculature is necessary to facilitate blood perfusion in the recellularized liver graft without blood clotting and leakage into the parenchymal space. Previously, researchers

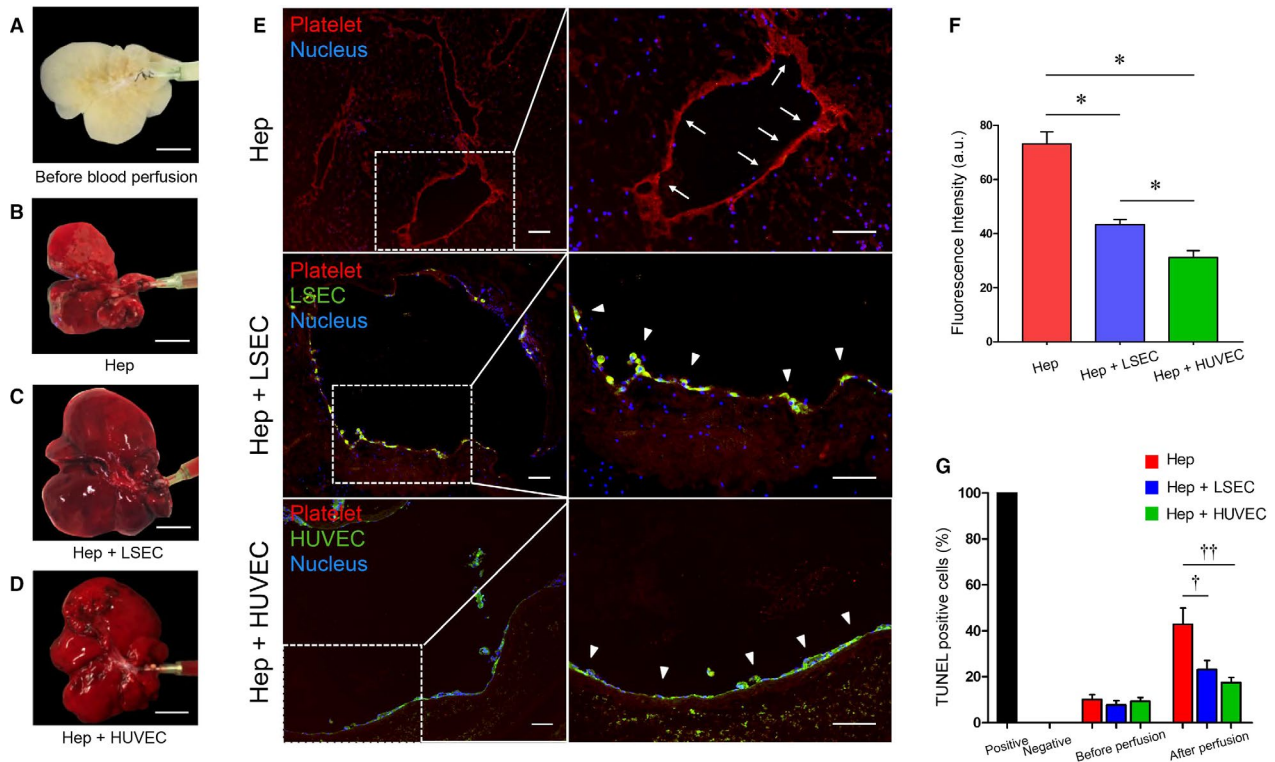


FIGURE 6 Functional LSECs and HUVECs in the recellularized liver graft during extracorporeal blood perfusion. Gross appearance of the recellularized liver graft before extracorporeal blood perfusion (A), and after 3 hours of extracorporeal perfusion with hepatocytes seeded alone (Hep) (B), together with LSECs (Hep + LSEC) (C), and together with HUVECs (Hep + HUVEC) (D). (E) Platelet deposition evaluated with integrin α IIb staining (arrows) in the Hep group (top), Hep + LSEC group (middle), and Hep + HUVEC group (bottom). Arrowheads indicate SE-1 expression in LSECs (middle) and CD31 expression in HUVECs (bottom) after extracorporeal blood perfusion. (F) Quantification of platelet deposition based on the average fluorescence intensities of integrin α IIb. (G) Number of TUNEL-positive hepatocytes before and after extracorporeal perfusion in the 3 groups. Scale bars = 10 mm (A–D) and 100 μ m (E). All error bars represent the standard error of the mean ($n = 3$). * $P < .001$, † $P = .027$, †† $P = .004$; a.u., arbitrary unit [Colour figure can be viewed at wileyonlinelibrary.com]

transplanted decellularized liver grafts with or without endothelial cells and evaluated the effects on platelet deposition.^{4,11} These studies demonstrated a significant role for endothelial cells in reducing platelet deposition in the scaffold without parenchymal cells. Here, we demonstrated reduced platelet deposition in liver recellularized concomitantly with endothelial and parenchymal cells. To the best of our knowledge, no study has previously evaluated blood clotting in a scaffold recellularized with parenchymal cells in addition to endothelial cells. This is due to the difficulty in vascularizing a decellularized liver while simultaneously reproducing the parenchyma in their appropriate locations. The problem was partially resolved by repopulating endothelial cells along the portal tree via PV seeding as well as introduction of hepatocytes into the parenchymal space via BD seeding. Our seeding method could help produce a practical recellularized liver graft with hepatic function under blood perfusion conditions.

Because of their antithrombogenicity, endothelial cells reduced thrombus formation and contributed to maintaining hepatocyte viability in the extracorporeal blood perfusion system. In anticipation of a clinical application, we conducted a preliminary evaluation of the feasibility of our recellularized livers in extracorporeal perfusion for 8 hours. The rats could tolerate 8 hours of extracorporeal perfusion with no death recorded over the long-term after the procedure. Indeed, we successfully achieved continuous blood flow into the vascularized liver

graft by extracorporeal perfusion for at least 8 hours. This suggests that use of re-endothelialized liver with extracorporeal perfusion might improve the hemocompatibility of a decellularized liver graft. Our findings open the possibility of using recellularized livers with extracorporeal perfusion to support patients with posthepatectomy liver failure or patients with end-stage liver disease as a bridge to transplantation.

Primary hepatocytes and LSECs tend to rapidly lose their original morphology and function after isolation.^{26,27} In the present study, we demonstrated fenestrations in addition to SE-1 and stabilin-2 expression, indicating that LSECs maintained their morphology and phenotype on the vasculature of the decellularized liver. DPPIV staining suggested proper configuration of bile canaliculi in the parenchyma. Furthermore, hepatocytes co-cultured with LSECs significantly retained their performance in the present engineered 3D liver. Although we could not completely cover the hepatocytes with LSECs via sinusoids, the attached LSECs might affect the maintenance of hepatocyte function through contact via the portal lumen and soluble factors secreted by endothelial cells.²⁸ Liver-specific ECM-to-liver cell interactions as well as cell-to-cell interactions between hepatocytes and LSECs might have contributed to maintaining their function, phenotype, and morphology in our study. Our approach provides insight into the development of recellularized liver grafts with better hepatic function for liver support, and the cell sources required for efficient recellularization.

Besides LSECs, we used another vascular endothelial cell source, HUVECs, as a comparison. Although HUVECs tended to maintain hepatocyte function, especially in terms of albumin secretion and suppressed thrombus formation, more successfully than LSECs, the latter were nevertheless better at maintaining hepatic function. Further studies are required to investigate the most adequate endothelial cell source to ensure proper hepatic function of recellularized liver grafts under blood perfusion.

In conclusion, our proposed seeding method provided optimal cell distribution into the parenchyma as well as the vasculature following the 3D structure of the decellularized liver. LSECs supported hepatocyte viability under blood perfusion, maintaining hepatocyte function and suppressing thrombus formation in the engineered liver graft. The recellularization procedure described in this study is expected to help produce functional liver grafts under blood perfusion.

ACKNOWLEDGMENTS

This work was supported by grants from the Japan Society for the Promotion of Science (Grant 15K15065).

DISCLOSURE

The authors of this manuscript have no conflicts of interest to disclose as described by the *American Journal of Transplantation*.

REFERENCES

- Dhawan A, Puppi J, Hughes RD, Mitry RR. Human hepatocyte transplantation: current experience and future challenges. *Nat Rev Gastroenterol Hepatol*. 2010;7(5):288-298.
- Stockmann HB, Hiemstra CA, Marquet RL, JN IJ. Extracorporeal perfusion for the treatment of acute liver failure. *Ann Surg*. 2000;231(4):460-470.
- Uygun BE, Soto-Gutierrez A, Yagi H, et al. Organ reengineering through development of a transplantable recellularized liver graft using decellularized liver matrix. *Nat Med*. 2010;16(7):814-820.
- Baptista PM, Siddiqui MM, Lozier G, Rodriguez SR, Atala A, Soker S. The use of whole organ decellularization for the generation of a vascularized liver organoid. *Hepatology*. 2011;53(2):604-617.
- Soto-Gutierrez A, Zhang L, Medberry C, et al. A whole-organ regenerative medicine approach for liver replacement. *Tissue Eng Part C Methods*. 2011;17(6):677-686.
- Handa K, Matsubara K, Fukumitsu K, Guzman-Lepe J, Watson A, Soto-Gutierrez A. Assembly of human organs from stem cells to study liver disease. *Am J Pathol*. 2014;184(2):348-357.
- Soto-Gutierrez A, Wertheim JA, Ott HC, Gilbert TW. Perspectives on whole-organ assembly: moving toward transplantation on demand. *J Clin Invest*. 2012;122(11):3817-3823.
- Yagi H, Fukumitsu K, Fukuda K, et al. Human-scale whole-organ bioengineering for liver transplantation: a regenerative medicine approach. *Cell Transplant*. 2013;22(2):231-242.
- Ogiso S, Yasuchika K, Fukumitsu K, et al. Efficient recellularisation of decellularised whole-liver grafts using biliary tree and foetal hepatocytes. *Sci Rep*. 2016;6:35887.
- Kadota Y, Yagi H, Inomata K, et al. Mesenchymal stem cells support hepatocyte function in engineered liver grafts. *Organogenesis*. 2014;10(2):268-277.
- Ko IK, Peng L, Peloso A, et al. Bioengineered transplantable porcine livers with re-endothelialized vasculature. *Biomaterials*. 2015;40:72-79.
- Bruinsma BG, Kim Y, Berendsen TA, Ozer S, Yarmush ML, Uygun BE. Layer-by-layer heparinization of decellularized liver matrices to reduce thrombogenicity of tissue engineered grafts. *J Clin Transl Res*. 2015;1(1). pii: 04
- Zhou P, Huang Y, Guo Y, et al. Decellularization and recellularization of rat livers with hepatocytes and endothelial progenitor cells. *Artif Organs*. 2016;40(3):E25-E38.
- Rieder H, Meyer zum Buschenfelde KH, Ramadori G. Functional spectrum of sinusoidal endothelial liver cells. Filtration, endocytosis, synthetic capacities and intercellular communication. *J Hepatol*. 1992;15(1-2):237-250.
- Fraser R, Dobbs BR, Rogers GW. Lipoproteins and the liver sieve: the role of the fenestrated sinusoidal endothelium in lipoprotein metabolism, atherosclerosis, and cirrhosis. *Hepatology*. 1995;21(3):863-874.
- McCuskey RS. The hepatic microvascular system in health and its response to toxicants. *Anat Rec (Hoboken)*. 2008;291(6):661-671.
- Limmer A, Ohl J, Kurts C, et al. Efficient presentation of exogenous antigen by liver endothelial cells to CD8+ T cells results in antigen-specific T-cell tolerance. *Nat Med*. 2000;6(12):1348-1354.
- Bale SS, Golberg I, Jindal R, et al. Long-term coculture strategies for primary hepatocytes and liver sinusoidal endothelial cells. *Tissue Eng Part C Methods*. 2015;21(4):413-422.
- Kita S, Yasuchika K, Ishii T, et al. The protective effect of transplanting liver cells into the mesentery on the rescue of acute liver failure after massive hepatectomy. *Cell Transplant*. 2016;25(8):1547-1559.
- March S, Hui EE, Underhill GH, Khetani S, Bhatia SN. Microenvironmental regulation of the sinusoidal endothelial cell phenotype in vitro. *Hepatology*. 2009;50(3):920-928.
- Stefanovich P, Matthew HW, Toner M, Tompkins RG, Yarmush ML. Extracorporeal plasma perfusion of cultured hepatocytes: effect of intermittent perfusion on hepatocyte function and morphology. *J Surg Res*. 1996;66(1):57-63.
- Thomas C, Pellicciari R, Pruzanski M, Auwerx J, Schoonjans K. Targeting bile-acid signalling for metabolic diseases. *Nat Rev Drug Discov*. 2008;7(8):678-693.
- Barakat O, Abbasi S, Rodriguez G, et al. Use of decellularized porcine liver for engineering humanized liver organ. *J Surg Res*. 2012;173(1):e11-e25.
- Mazza G, Rombouts K, Rennie Hall A, et al. Decellularized human liver as a natural 3D-scaffold for liver bioengineering and transplantation. *Sci Rep*. 2015;5:13079.
- Verstegen MMA, Willemsse J, van den Hoek S, et al. Decellularization of whole human liver grafts using controlled perfusion for transplantable organ bioscaffolds. *Stem Cells Dev*. 2017;26(18):1304-1315.
- Sellaro TL, Ravindra AK, Stolz DB, Badylak SF. Maintenance of hepatic sinusoidal endothelial cell phenotype in vitro using organ-specific extracellular matrix scaffolds. *Tissue Eng*. 2007;13(9):2301-2310.
- Sellaro TL, Ranade A, Faulk DM, et al. Maintenance of human hepatocyte function in vitro by liver-derived extracellular matrix gels. *Tissue Eng Part A*. 2010;16(3):1075-1082.
- Jindal R, Nahmias Y, Tilles AW, Berthiaume F, Yarmush ML. Amino acid-mediated heterotypic interaction governs performance of a hepatic tissue model. *FASEB J*. 2009;23(7):2288-2298.

SUPPORTING INFORMATION

Additional Supporting Information may be found online in the supporting information tab for this article.

How to cite this article: Kojima H, Yasuchika K, Fukumitsu K, et al. Establishment of practical recellularized liver graft for blood perfusion using primary rat hepatocytes and liver sinusoidal endothelial cells. *Am J Transplant*. 2018;18:1351-1359. <https://doi.org/10.1111/ajt.14666>